Community function landscape and steady state species ratio shape the eco-evolutionary dynamics of artificial community selection

Li Xie[1*] **and Wenying Shou**[1*]

[1]Division of Basic Sciences, Fred Hutchinson Cancer Research Center, Seattle, WA, USA

***For correspondence:**
xie-li@outlook.com (LX);
wenying.shou@gmail.com (WS)

Abstract How might we artificially select multi-species microbial communities to improve their functions? In the accompanying article, we have modeled a commensal community where Helper releases Byproduct essential to Manufacturer, and Manufacturer diverts a fraction f_P of its growth to make Product. Low-density "Newborn communities" grow and mutate over time T into "Adult communities", and Adult communities with the highest function (total Product) are randomly partitioned into Newborn communities of the next cycle. Here, to understand selection dynamics, we visualize community function landscape ("landscape") which relates community phenotype composition (e.g. species ratio; Manufacturer's f_P) to community function. We show that although an interaction can enable species coexistence by driving species ratio toward an "attractor", it can constrain selection if maximal function lies outside of the attractor. Landscape-attractor diagrams allow us to evaluate the effectiveness of different selection regimens, including screening communities comprising one random clone from each species.

Introduction

Multi-species microbial communities often display *community functions* - biochemical activities not achievable by any member species alone. For example, a community of *Desulfovibrio vulgaris* and *Methanococcus maripaludis*, but not either species alone, converts lactate to methane in the absence of sulfate ***Hillesland and Stahl*** (***2010***). Community function may be improved by artificial selection. That is, newly-assembled "Newborn communities" ("Newborns") grow and mutate during "maturation time" T to become "Adult communities" ("Adults"). Adults expressing the highest community functions are selected to "reproduce" where each is randomly partitioned into multiple Newborns for the next selection cycle. Artificial community selection, if successful, can improve useful community functions such as fighting pathogens ***Lawley et al.*** (***2012***), producing drugs ***Zhou et al.*** (***2015***), or degrading wastes ***Kato et al.*** (***2004***). However, compared to selection on individuals, selection on communities is less likely to succeed (Figure 1 of accompanying article).

We have simulated artificial selection on a Helper-Manufacturer community (see accompanying article for model details and their experimental justifications). In this community, Helper H consumes excess Waste and releases Byproduct B essential to Manufacturer M, while M diverts a fraction f_P of its growth resource to make Product P. H and M additionally compete for a shared Resource R. Community function $P(T)$ is the total amount of Product accumulated as a Newborn community matures over time T to become an Adult community. We choose the number of population doublings within T to be relatively small to prevent any newly-arising mutants from taking

over. Thus, community function at adulthood is mostly determined by compositions of species and their genotypes at the Newborn stage ("Newborn composition").

To reduce the dimension of our problem, we have chosen model parameters such that improving H and M's maximal growth rates and affinities for required nutrients increases community function. Thus, we can fix these growth phenotypes at their respective evolutionary upper bounds, since mutants that reduce these phenotypes will be selected against by both natural selection and community selection. Consequently, we only need to focus on one evolvable phenotype: Manufacturer's f_P.

Maximal community function is achieved at an intermediate f_P. This is because at $f_P = 0$, no Product is made, while at $f_P = 1$, M does not grow and is out-competed by H. Natural selection will favor lower f_P. Thus, even when we start with the f_P optimal for community function ($f_P^* = 0.41$), it and community function will decline in the absence of community selection.

Can community selection counter natural selection to increase f_P and thus community function? We have shown that the answer depends on community selection regimen (accompanying article). Let's consider the case where we supply excess Resource to prevent stationary phase. If we reproduce an Adult community by pipetting a portion of it into each Newborn, then Newborn composition in terms of total biomass $N(0)$ and fraction of M biomass $\phi_M(0)$ fluctuates, which interferes with community selection. In other words, an Adult community may be selected not because of mutations that increase the average f_P among Manufacturers, but because its composition at the newborn stage happens to favor community function. In contrast, if we sort fixed H and M biomass or cell number into each Newborn, community function improves but curiously does not reach the theoretical maximum.

How might we understand selection dynamics under different selection regimens? Here, we visualize "community function landscape" together with "species composition attractor". We show how such visualization helps us understand ecological-evolutionary dynamics during artificial community selection.

Results

Visualizing community function landscape and species composition attractor

A landscape graphically represents how a quantity of interest varies across the composition space of a system. For example, in evolutionary biology, phenotype-fitness landscape represents the fitness of an individual as a function of its phenotypic values ***Lunzer et al.*** (***2005***). When many phenotypes jointly determine fitness, phenotype-fitness landscape is hyper-dimensional and thus difficult to visualize. However, we can reduce the dimension by fixing all phenotypes of an individual except for its maximal growth rate and nutrient affinity for the limiting metabolite. In this case, growth rate g may be expressed by Monod kinetics $g = g_{max}\frac{c}{c+K}$ where c is the concentration of the limiting metabolite, g_{max} is the individual's maximal growth rate, and K is the metabolite concentration at which half maximal growth rate is achieved. g can be visualized by a 3D plot as a function of g_{max} and K/c (***Figure 1–Figure Supplement 1***). This landscape illustrates that higher g is attained at higher g_{max} and lower K.

To understand selection dynamics in the Helper-Manufacturer community, we want to visualize its "community function landscape" (short-handed as "landscape"). At a fixed maturation time T and initial Resource, community function $P(T)$ depends on initial conditions and parameters (species phenotypes) of our model. Initial conditions include a Newborn community's total biomass $N(0)$ and fraction M biomass $\phi_M(0)$. Species phenotypes include H and M's growth phenotypes (maximal growth rates; affinities for metabolites) and f_P, the fraction of M's growth resource diverted to making Product. As described in Introduction, we have fixed all growth parameters to their respective evolutionary upper bounds, and only allow Manufacturer's f_P to vary. During community reproduction, $N(0)$ and $\phi_M(0)$ can fluctuate stochastically.

We have chosen a sufficiently short T such that within a selection cycle, newly-arising mutations

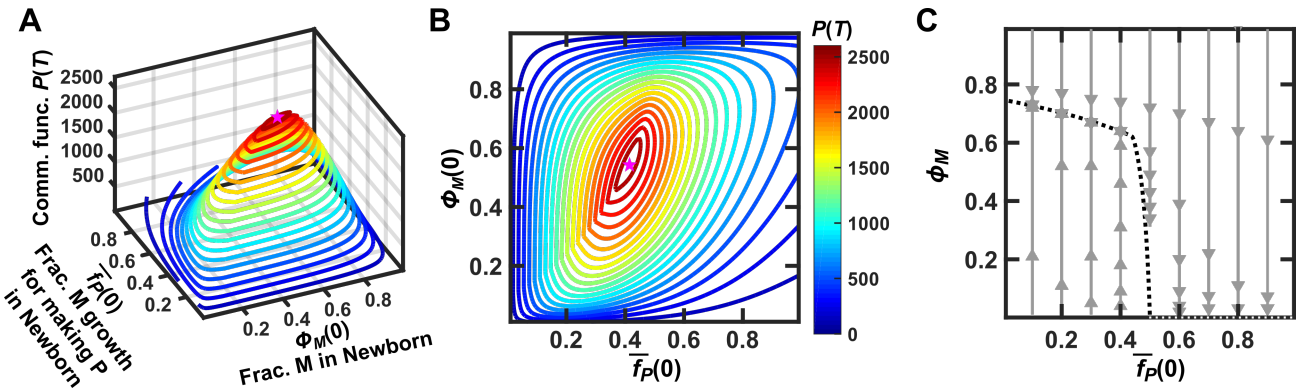

Figure 1. Visualizing community function landscape ("landscape") and species composition attractor ("attractor"). (**A**) A 3D plot of community function $P(T)$ as a function of $\overline{f}_P(0)$ and $\phi_M(0)$. $P(T)$ is calculated assuming that all Manufactures have the same f_P ($\overline{f}_P(0)$) and that the effects of new mutations arising during maturation are negligible. (**B**) Contour plot of **A**. The magenta star in A and B marks the position of global maximal $P(T)$. In our parameter space, a single maximal $P(T)$ occurs at $f_P^*(0) = 0.41$ and $\phi_M^*(0) = 0.54$. (**C**) Species composition attractor. At various fixed f_P, each grey arrow starts at ϕ_M of a Newborn community and ends at ϕ_M of the Adult community after maturation time T. The dotted line is the attractor.

Figure 1–Figure supplement 1. Fitness landscape of growth rate g at a fixed metabolite concentration.

in f_P do not have enough time to rise to a sufficiently high frequency to impact community function. If we additionally fix the total biomass of a Newborn, then community function $P(T)$ depends only on Newborn's fraction of M biomass $\phi_M(0)$ and M's f_P. As we demonstrate below (***Figure 3–Figure Supplement 2***), the latter term can be approximated as $\overline{f}_P(0)$, f_P averaged over all M in a Newborn community. Thus, landscape can be visualized as Figure 1A. We further flatten community function landscape to a 2D contour plot (Figure 1B), and use color to indicate community function. As evident from the landscape diagram, maximal community function (magenta star in Figure 1A and B) is achieved at an intermediate $\overline{f}_P(0)$ and $\phi_M(0)$.

As we have shown (accompanying article Figure 3), $\overline{f}_P(0)$ affects ϕ_M. At high $\overline{f}_P(0)$, M has low growth rate and eventually goes extinct ($\phi_M = 0$; white dotted line on the *x*-axis in Figure 1C). At low $\overline{f}_P(0)$, $\phi_M(T)$ reaches a non-zero steady state value $\phi_{M,SS}$ (black dotted line in Figure 1C). $\phi_{M,SS}$ values at various $\overline{f}_P(0)$ form a species composition attractor (short-handed as "attractor"): ϕ_M values away from the attractor will always move rapidly toward the attractor compared to how fast $\overline{f}_P(0)$ evolves. This attractor is a consequence of the commensal interaction between H and M ***Momeni et al.*** (***2013***).

Both the landscape and the attractor govern community selection. Since species composition will always be pulled toward the attractor, successful community selection will push community function up the landscape along the attractor. We can thus superimpose the two graphs to visualize selection dynamics, as we demonstrate in Figure 2B.

Attractor can constrain community selection

Community function sometimes fails to reach the maximum despite community selection. For example, let's consider the following selection scheme. We start from 100 Newborn communities, each containing 40 H cells each of biomass 1, and 60 M cells each of biomass 1 and $f_P = 0.13$. On average, Resource R is in moderate (~30%) excess by the end of T to avoid stationary phase. During T, each M and H cell takes up required metabolites (H consumes Resource, and M consumes Resource and H's Byproduct), and increases in biomass. Once the biomass of a cell reaches the threshold of 2, the cell divides into two cells of equal biomass. f_P-altering mutations arise stochastically at a rate achievable in hyper-mutators (2×10^{-3}/cell/generation). How mutations affect f_P is based on experimental observations: half of the mutations generate non-producers ($f_P = 0$), while the other half increase or decrease f_P by an average of 5~6% (Fig 4 of accompanying article). At the end of T, we select the Adult community with the highest $P(T)$ to reproduce by

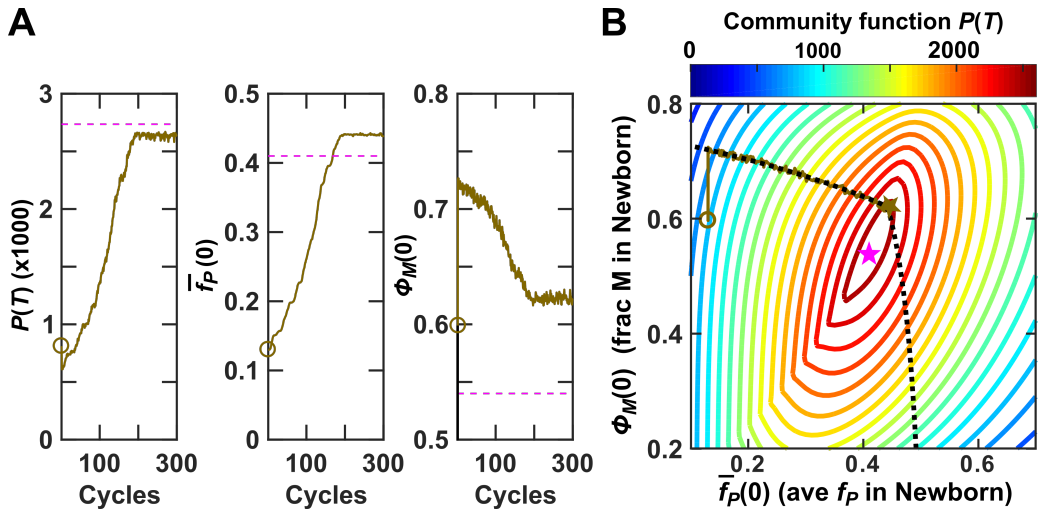

Figure 2. Community selection dynamics on the landscape-attractor diagram. (**A**) Dynamics during community selection. Magenta dashed lines mark values corresponding to the global maximal $P(T)$ where $T = 17$. (**B**) Community function landscape superimposed with steady state composition attractor (black dotted line). The large open circle marks Newborn composition $\left\{\overline{f}_P(0), \phi_M(0)\right\}$ for the 1st cycle. Olive-colored curve corresponds to evolutionary dynamics as shown in (A). Magenta and olive stars respectively correspond to community compositions for maximal $P(T)$ in theory and in practice.

"sorting" biomass so that each Newborn has a total biomass near the target $N_0 = 100$, with species composition similar to that of the parent Adult. In practice, cell biomass can be measured by, for example, fluorescence intensity. When the top-functioning Adult is depleted, we use the second highest-functioning Adult until we obtain a total of 100 Newborns (see details of the simulation code in accompanying article).

Under this selection regime, community function improves but levels off at sub-maximum (Fig 2A, left panel). $\overline{f}_P(0)$, the average f_P of Manufactures in successful Newborns that will get selected at adulthood, exceeds what is required for maximal $P(T)$ (Fig 2A, middle panel). This is surprising since Manufactures with lower f_P grow faster. Then, why would successful Newborn communities end up with f_P neither favored by community selection nor by natural selection?

The answer becomes clear when we plot evolutionary dynamics on the landscape-attractor diagram (Figure 2B). Starting from the open circle, olive dots mark the average composition of successful Newborns over successive cycles. Within the first cycle, $\overline{f}_P(0)$ barely changes due to the rarity of mutations and the lack of time for any new mutation to rise to high frequency within T. $\phi_M(0)$, fraction M in Newborn, quickly reaches the steady state value on the attractor (Figure 2B, black dotted line). Afterwards, species composition is always constrained to near the attractor as $\overline{f}_P(0)$ improves. Since the attractor does not pass through maximal community function (Figure 2B, magenta star), community function is sub-maximal (Figure 2B, olive star). The geometry of the landscape-attractor diagram further reveals that the final selected $\overline{f}_P(0)$ overshoots the value required for maximal community function (Figure 2B, olive star to the right of magenta star). The final $\phi_M(0)$ also exceeds that required for maximal community function (Figure 2B, olive star above magenta star).

Visualizing the effectiveness of community selection regimens

In this section, we demonstrate how landscape-attractor diagrams, together with the statistical distribution of Newborn composition, can be used to qualitatively evaluate the effectiveness of selection regimens.

Let's consider selection regimens where $N(0)$ is fixed but $\phi_M(0)$ is allowed to fluctuate stochastically during community reproduction. Experimentally, this corresponds to fixing Newborn turbidity.

At fixed $N(0)$, community function landscape can be visualized as a 2D diagram with $\phi_M(0)$ and $f_P(0)$ as the two variables (Figure 2B). We already know that community function barely improves at maturation time $T = 17$ ("short T") but improves rapidly when T increases to 20 ("long T") (Figure 7 in accompanying article). We will now explain this difference by comparing their landscape-attractor diagrams.

Short T and long T generate similar landscape-attractor diagrams at the global scale (***Figure 3–Figure Supplement 1***). However when we zoom into the scale where mutation operates (i.e. a few percent of the ancestral f_P), differences emerge (Figure 3). To see this difference, let's consider two consecutive selection cycles. We start with $n_{tot} = 100$ Newborn communities, with their $\{\overline{f}_P(0), \phi_M(0)\}$ compositions marked as open circles (Panel i of Figure 3A, C). Strictly speaking, $P(T)$ is determined by the time-dependent f_P distribution as well as the dynamics of H and M in a community throughout maturation time T. However, because T is sufficiently short to prevent new mutations from rising to a high frequency within a cycle, $P(T)$ can be adequately predicted from Newborn compositions $\{\overline{f}_P(0), \phi_M(0)\}$ (***Figure 3–Figure Supplement 2***) using Eqs. 1-5. In other words, when reaching adulthood, a Newborn will achieve community function as indicated by the color of the community function isocline it sits on. We mark the $\overline{f}_P(0)$ averaged among all Newborn communities of the first cycle as a reference (grey dashed line).

Out of the 100 Newborns, two will be "successful" (magenta open circles) in the sense that they will achieve the highest community function at adulthood and reproduce. Graphically, successful Newborns occupy the yellowest region of the landscape (Panel i of Figure 3A, C). By time T (filled circles in Panel ii of Figure 3A, C), $\overline{f}_P(T)$ has declined due to the fitness advantage of Manufacturers with lower f_P, and $\phi_M(T)$ has reached the steady state $\phi_{M,SS}$. The two successful Adult communities are then partitioned randomly into a total of $n_{tot} = 100$ Newborn communities (Panel iii of Figure 3A, C).

When T is short, we sometimes end up selecting communities with sub-optimal $\overline{f}_P(0)$ (Figure 3A, magenta circles to the left of the dashed reference) if their $\phi_M(0)$ values happen to promote $P(T)$. In contrast, when T is long, all selected communities have high $\overline{f}_P(0)$ (Figure 3 C). This trend becomes even more apparent when we examine the statistical outcome of community reproduction and selection in repeated trials: $\overline{f}_P(0)$ of successful Newborns (cloud of magenta circles in Figure 3B and D) show improvement over the reference when T is long but not when T is short. This difference can be explained by examining the landscape geometry below the attractor where higher community function resides: the isoclines are diagonal when T is short, whereas they are nearly vertical when T is long. Let's compare a small region of the landscape (purple rectangles in Figure 3A and C). In this region, an increase in $\overline{f}_P(0)$ improves $P(T)$ in a similar fashion for short and long T (i.e. improving by two isoclines as marked by two horizontal arrows). As $\phi_M(0)$ fluctuates in the vertical direction within the rectangle, $P(T)$ can change by 4 isoclines for short T, but barely changes for long T (vertical arrows). This difference translates to how fluctuations in $\phi_M(0)$ differentially interfere with community selection when T is short versus long, and consequently whether community selection will improve $\overline{f}_P(0)$ and $P(T)$.

Standard community selection can outperform combination screening

Instead of the standard community selection described above, we could screen combinations of clones, with each member species contributing a random clone ("combination screening"). For example to construct a Newborn community, we could grow one random clone per species, and mix them at a pre-fixed species ratio. We then select the highest-functioning Adult communities to reproduce: we plate them out, randomly choose one clone per member species, and mix them at the pre-fixed species ratio to form Newborns of the next cycle. Combination screening is a variation of community selection. One difference is that in combination screening, a Newborn community starts with a predetermined species ratio while in standard community selection, a Newborn inherits the species ratio of the parent community.

Let's consider the H-M community where H and M have been pre-optimized in monocultures.

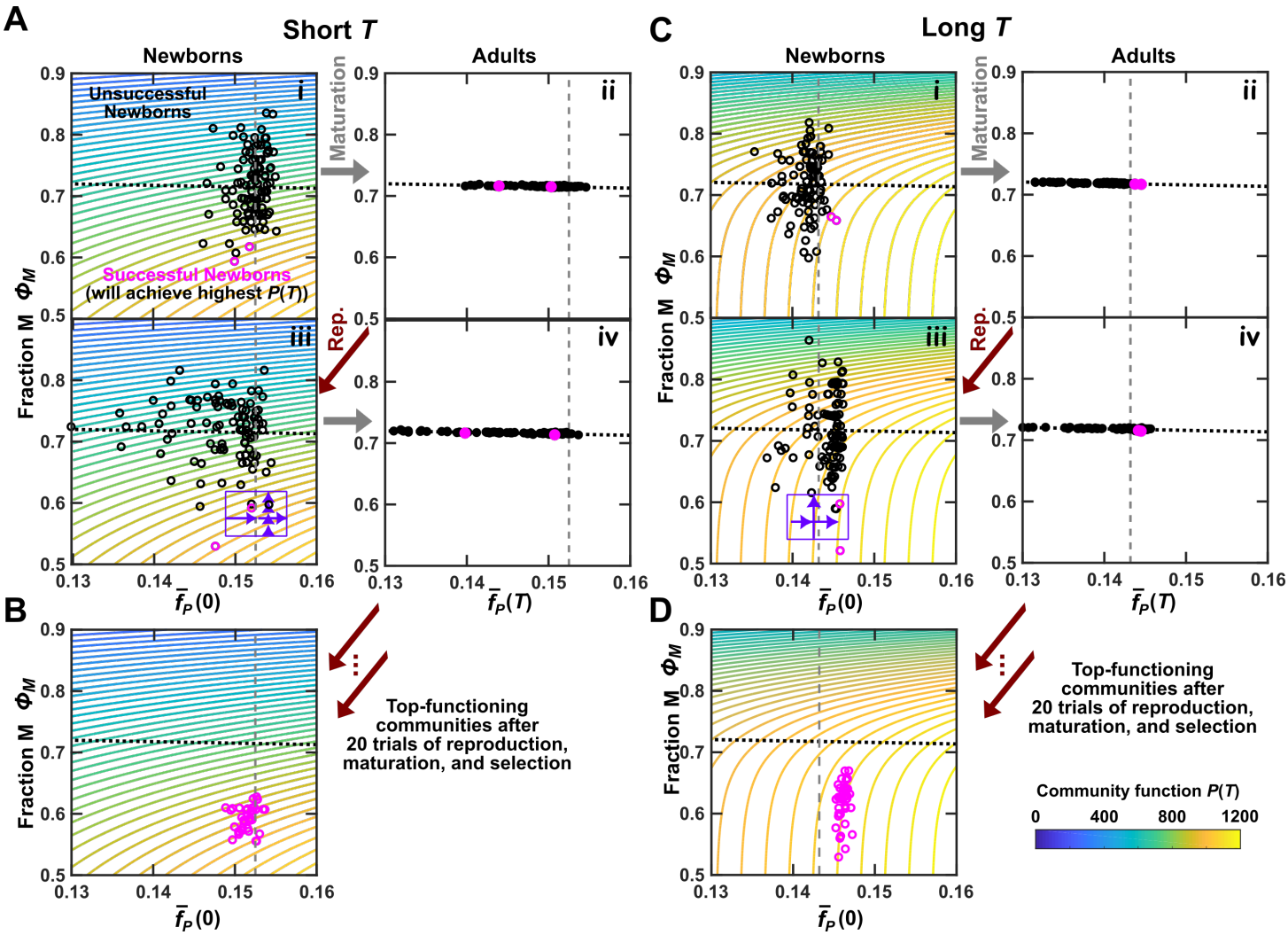

Figure 3. Landscape-attractor diagrams reveal the effectiveness of selection regimens. (**A, C**) (**i**): $\{\overline{f}_P(0), \phi_M(0)\}$ compositions of 100 Newborn communities from a selection cycle (open circles), with the two Newborns that will achieve the highest community function colored in magenta whereas the rest in black. Each color curve marks an isocline of a particular $P(T)$ value. The $\overline{f}_P(0)$ averaged across the 100 Newborns (grey dashed line) of the initial selection cycle serves as a reference for tracking improvements of $\overline{f}_P(0)$ and thus of community function in subsequent cycles. (**ii**): Compositions of Adult communities (solid circles). $\overline{f}_P(T)$ generally declines during maturation due to the fitness advantage of lower-producers, and $\phi_M(T)$ has converged to the attractor. Adult communities with the highest $P(T)$ (magenta) are selected to reproduce. (**iii**): Newborn communities of the subsequent cycle. (**iv**): Adult communities of the subsequent cycle. **Purple rectangles**: Arrows connect two adjacent $P(T)$ contours. Vertical arrows show that when T is short (but not when when T is long), fluctuations in $\phi_M(0)$ greatly affect community function. Horizontal arrows show that changes in $\overline{f}_P(0)$ affect $P(T)$ similarly for short or long T. In both (**A**) and (**C**), the purple rectangle is centered around the grey dashed reference line. (**B, D**) Adult communities in Panel iv of A and C are allowed to undergo reproduction, maturation, and selection (using the simulation code in accompanying article). To account for stochasticity in cell mutation and death and during community reproduction, we repeat this same simulation 20 times using different random number sequences. The statistical distributions of $\{\overline{f}_P(0), \phi_M(0)\}$ compositions of successful Newborns are plotted. $\overline{f}_P(0)$ improves over the reference when T is long, and barely improves when T is short. The interval between two adjacent contours is the same for short and long T.

Figure 3–Figure supplement 1. Landscape-attractor diagrams for short and long T appear similar at the global scale.

Figure 3–Figure supplement 2. $P(T)$ calculated from the differential equations agree well with those from stochastic simulations.

Figure 3–Figure supplement 3. Restricting fluctuations in $\phi_M(0)$ facilitates community selection.

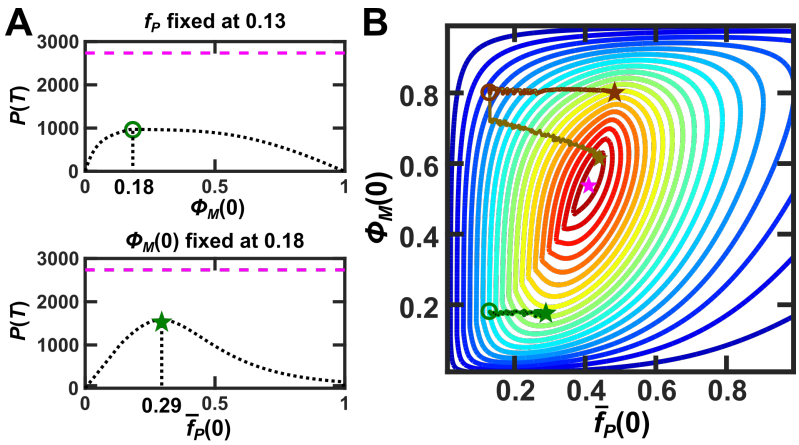

Figure 4. Combination screening fixated at a pre-deter mined $\phi_M(0)$ may significantly under-shoot theoretical maximal community function. (**A**) Top: At the initial stage where $f_P = 0.13$, maximal $P(T)$ is achieved at $\phi_M(0) = 0.18$. Bottom: If community selection is performed at fixed $\phi_M(0) = 0.18$, maximal $P(T)$ (green star) is only about half of the theoretical maximal (magenta dashed line). $P(T)$ is calculated from differential equations assuming that all M share identical f_P. (**B**) Selection dynamics is plotted on community function landscape, with contour color scale identical to that in Figure 1. Evolutionary dynamics during standard selection (olive) and combination screening (brown and green) are plotted, with circles and stars respectively mark the beginning and the maximal $P(T)$ of community selection. Olive and brown trajectories share the same starting point. Here, $N(0)$=100 biomass units.

Figure 4–Figure supplement 1. Combination screening at a pre-fixed $\phi_M(0)$ can underperform or outperform standard community selection where a Newborn inherits the species ratio of its parent Adult.

Since H is already fixed at its evolutionary upper bound, combination screening will involve fixed H but variable M. An experimentalist starts with $f_P = 0.13$ (f_P of pre-optimized M, see accompanying article), and by trying different H:M ratios, realizes that maximal community function is achieved at $\phi_M(0)$ of 0.18 (green circle in Figure 4A top panel and Figure 4B). If the experimentalist fixes $\phi_M(0)$ to 0.18, community selection could improve f_P to 0.29 where community function $P(T)$ is only about half of the theoretical maximal (green star in Figure 4A bottom panel and Figure 4B), much lower than the maximal $P(T)$ achieved in standard selection (Figure 4B olive trajectory). In general, from the same starting ratio, standard selection will outperform combination screening if as f_P improves, species composition attractor changes in the direction that promotes community function (Figure 4B, olive trajectory outperforming brown trajectory). If the experimentalist fixes $\phi_M(0)$ at a value near what is optimal for community function (e.g. 0.54), then combination screening will outperform standard selection (***Figure 4–Figure Supplement 1***). However, it is difficult to know a priori the species ratio corresponding to the maximal community function.

Discussion

To gain intuition about artificial selection of multi-species communities, we visualize community function landscape together with species composition attractor. In the H-M community, this is made possible by choosing model parameters and selection regimens so that community function varies with only two aspects of Newborn community composition — $\phi_M(0)$ (fraction M biomass) and $\overline{f}_P(0)$ (f_P averaged over all M in a Newborn community).

The landscape-attractor diagram illustrates that community selection can be constrained by ecological interactions between species. Species interactions such as commensalisms and mutualisms can facilitate species coexistence ***Shou et al.*** (***2007***); ***Momeni et al.*** (***2013***), giving rise to the attractor. However, this stability can constrain community selection if the maximal community function does not coincide with attractor (Figure 2B).

The local geometry of a landscape-attractor diagram, together with the statistical distribution of Newborn community composition, can lend intuitions to the effectiveness of a selection regimen

(Figure 3). For example in the H-M community, $P(T)$ can be affected by heritable variations in $\overline{f}_P(0)$ and by non-heritable fluctuations in $\phi_M(0)$ arising during community reproduction. Ideally, $P(T)$ improvement should be mainly driven by improving $\overline{f}_P(0)$. Since fluctuations in $\phi_M(0)$ affect community function less when T is long compared to when T is short (Figure 3, vertical arrows in the two purple rectangles), selection scheme with longer T is more effective in improving community function. If we want to keep T short, we can fix $\phi_M(0)$ by cell sorting. This regimen indeed improves community function (accompanying article Figure 7). Graphically speaking, this amounts to compressing the cloud of Newborn community compositions to a narrow band near the attractor (***Figure 3–Figure Supplement 3***). Now that fluctuations in $P(T)$ along $\phi_M(0)$ is much less than that along $\overline{f}_P(0)$, communities with higher $\overline{f}_P(0)$ get selected.

Using community function landscape diagram, we can compare the evolutionary dynamics of combination screening (where $\phi_M(0)$ is pre-fixed) with standard community selection (where $\phi_M(0)$ is inherited from the parent community). During standard selection, $\phi_M(0)$ stays near the attractor and can change in a direction that improves (***Figure 3–Figure Supplement 1***A) or diminishes (***Figure 3–Figure Supplement 1***B) community function. Combination screening can outperform standard selection if $\phi_M(0)$ is fixed at or near the value corresponding to maximal $P(T)$ (compare purple curve with olive curve in ***Figure 4–Figure Supplement 1***). Otherwise, standard community selection can outperform combination screening (Figure 4; compare olive curve with brown and blue curves in ***Figure 4–Figure Supplement 1***). Clearly, we can try alternative selection regimes. For example, we can start with standard selection, and once community function has reached a plateau, we can vary species ratio. If community function can be further improved by a new $\phi_M(0)$, we can continue selection while fixing $\phi_M(0)$ to this new value.

Combination screening can be applied to communities where species do not coexist over a prolonged time. Standard selection can also be applied to these communities if we re-adjust species ratio via cell sorting during community reproduction. For communities of three or more species, testing different species ratios during combination screening will be challenging. Any difficulties in culturing member species will add further challenges to combination screening, while standard selection does not require member species to be culturable.

An important difference emerges between combination screening and standard selection when intra-species interactions evolve. For example, M can evolve into two subpopulations, each carrying out a complementary module of Product biosynthesis. Interestingly, in at least some cases, partitioning a pathway into distinct cell populations has been demonstrated to enhance pathway activity ***Lilja and Johnson*** (***2016***); ***Zhang and Wang*** (***2016***), by for example, reducing enzyme competition for limited cofactors. Evolved intra-species interactions are precluded during combination screening (since we pick one clone per species), but can be selected for during standard community selection.

In general, community function landscape will be hyper-dimensional and difficult to visualize. However, we believe that the concept of community function landscape will be useful, much like the concept of "fitness landscape" ***Wright*** (***1932***).

Methods

Community function landscapes are plots of $P(T)$ numerically integrated from the following set of scaled differential equations (Eqs. 6-10 in accompanying article), assuming that all M cells have the same $f_P = \overline{f}_P(0)$:

$$\frac{dM}{dt} = g_M(R,\ B)\left(1 - f_P\right) M - \delta_M M \tag{1}$$

$$\frac{dH}{dt} = g_H(R)H - \delta_H H \tag{2}$$

$$\frac{dR}{dt} = -c_{RM} g_M(R,\ B)M - c_{RH} g_H(R)H \tag{3}$$

$$\frac{dB}{dt} = g_H(R)H - c_{BM}g_M(R,\ B)M \tag{4}$$

$$\frac{dP}{dt} = g_M(R,\ B)f_P M \tag{5}$$

where

$$g_H(R) = g_{Hmax}\frac{R}{R + K_{HR}}$$

$$g_M(R,\ B) = g_{Mmax}\frac{R_M B_M}{R_M + B_M}\left(\frac{1}{R_M + 1} + \frac{1}{B_M + 1}\right)$$

and $R_M = R/K_{MR}$ and $B_M = B/K_{MB}$. Definitions of all state variables and parameters are given in Table 1 of accompanying article. Parameters are from the "Mono-adapted" column of Table 1 of accompanying article.

Compositions of Newborn communities during community selection are results of stochastic, individual-based simulations. Details of the simulation code can be found in accompanying article. For Figure 3B and D, compositions of the two successful Newborn communities are plotted for each trial of community reproduction, maturation, and selection. This is repeated 20 times with the same Adult communities but with different random number sequences, resulting in a total of 40 Newborn compositions in Figure 3B and D.

Acknowledgments

Tony Long (UC Irvine) inspired the last section of this paper during the 2017 "Eco-Evolutionary Dynamics in Nature and the Lab" workshop at Kavli Institute of Theoretical Physics, UC Santa Barbara. We thank Alex Yuan (UW Seattle), Joan Strassmann (Wash U St. Louis), Bill Hazelton, Samuel Hart, and David Skelding for discussions. This research was supported by the High Performance Computing Shared Resource of the Fred Hutch Cancer Consortium (P30 CA015704).

References

Hillesland KL, Stahl DA. Rapid evolution of stability and productivity at the origin of a microbial mutualism. Proceedings of the National Academy of Sciences. 2010; 107(5):2124–2129.

Kato S, Haruta S, Cui ZJ, Ishii M, Igarashi Y. Effective cellulose degradation by a mixed-culture system composed of a cellulolytic Clostridium and aerobic non-cellulolytic bacteria. FEMS Microbiology Ecology. 2004; 51(1):133–142.

Lawley TD, Clare S, Walker AW, Stares MD, Connor TR, Raisen C, Goulding D, Rad R, Schreiber F, Brandt C, Deakin LJ, Pickard DJ, Duncan SH, Flint HJ, Clark TG, Parkhill J, Dougan G. Targeted restoration of the intestinal microbiota with a simple, defined bacteriotherapy resolves relapsing Clostridium difficile disease in mice. PLoS pathogens. 2012; 8(10):e1002995.

Lilja EE, Johnson DR. Segregating metabolic processes into different microbial cells accelerates the consumption of inhibitory substrates. The ISME Journal. 2016 Jul; 10(7):1568–1578. http://www.nature.com/ismej/journal/v10/n7/full/ismej2015243a.html, doi: 10.1038/ismej.2015.243.

Lunzer M, Miller SP, Felsheim R, Dean AM. The biochemical architecture of an ancient adaptive landscape. Science. 2005; 310(5747):499–501.

Momeni B, Brileya KA, Fields MW, Shou W. Strong inter-population cooperation leads to partner intermixing in microbial communities. eLife. 2013 Jan; 2. http://elifesciences.org/content/2/e00230.abstract, doi: 10.7554/eLife.00230.

Shou W, Ram S, Vilar JMG. Synthetic cooperation in engineered yeast populations. Proceedings of the National Academy of Sciences of the United States of America. 2007 Feb; 104(6):1877–1882. doi: 10.1073/pnas.0610575104, 00137.

Wright S. The roles of mutation, inbreeding, crossbreeding and selection in evolution. Proceedings of the Sixth International Congress of Genetics. 1932; 1:356–366.

Zhang H, Wang X. Modular co-culture engineering, a new approach for metabolic engineering. Metabolic Engineering. 2016 Sep; 37:114–121. http://www.sciencedirect.com/science/article/pii/S1096717616300180, doi: 10.1016/j.ymben.2016.05.007.

Zhou K, Qiao K, Edgar S, Stephanopoulos G. Distributing a metabolic pathway among a microbial consortium enhances production of natural products. Nature biotechnology. 2015; .

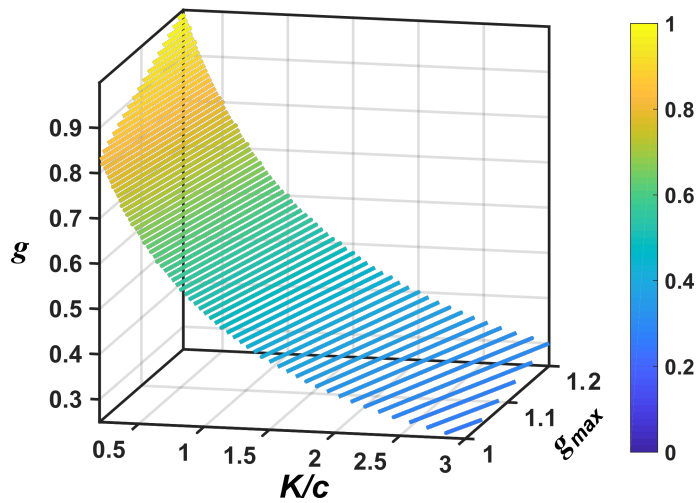

Figure 1–Figure supplement 1. Fitness landscape of growth rate g at a fixed metabolite concentration c. g is a function of maximal growth rate g_{max} and Monod constant K (concentration of metabolite at which half-maximal growth rate is achieved) according to the Monod kinetics. The highest growth rate (high g, yellow) is achieved at the lowest K and the highest g_{max} that are permitted by biology.

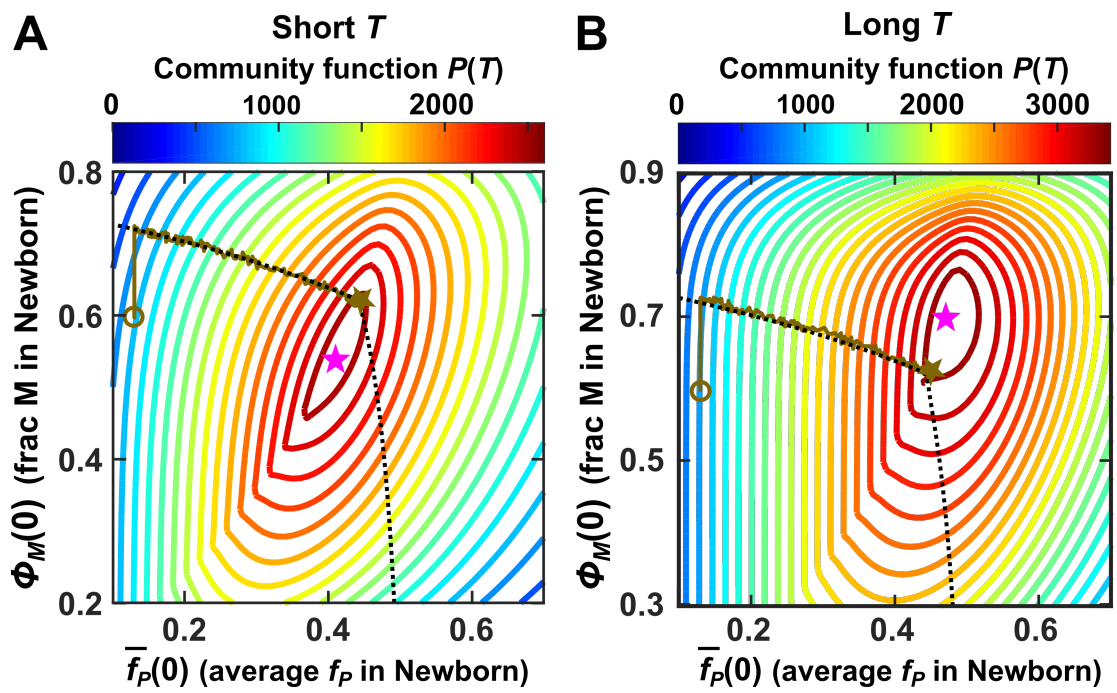

Figure 3–Figure supplement 1. Landscape-attractor diagrams for short and long T appear similar at the global scale. The magenta star marks the position of global maximal $P(T)$. The olive star marks the maximal $P(T)$ achieved by standard community selection.

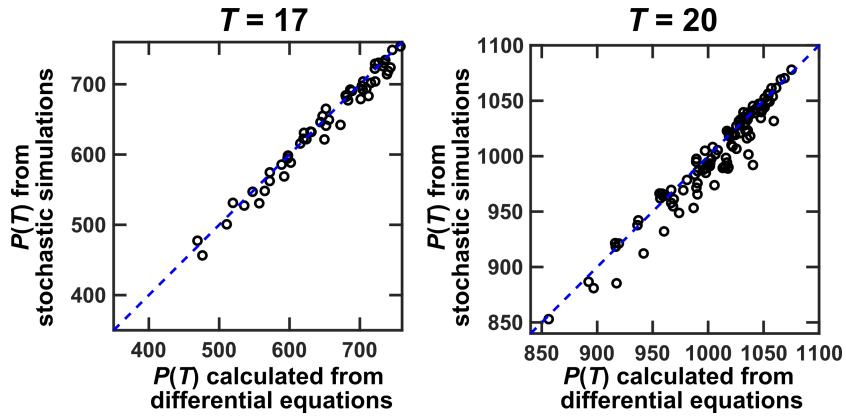

Figure 3–Figure supplement 2. $P(T)$ calculated from the differential equations agree well with those from stochastic simulations. $P(T)$ values are obtained from individual-based stochastic simulations where mutants are explicitly tracked. In parallel, $P(T)$ values are calculated from the differential equations using $\overline{f}_P(0)$ (Eqs. 1-5). The two sets of $P(T)$ values correlate well (the blue dashed line having a slope of 1).

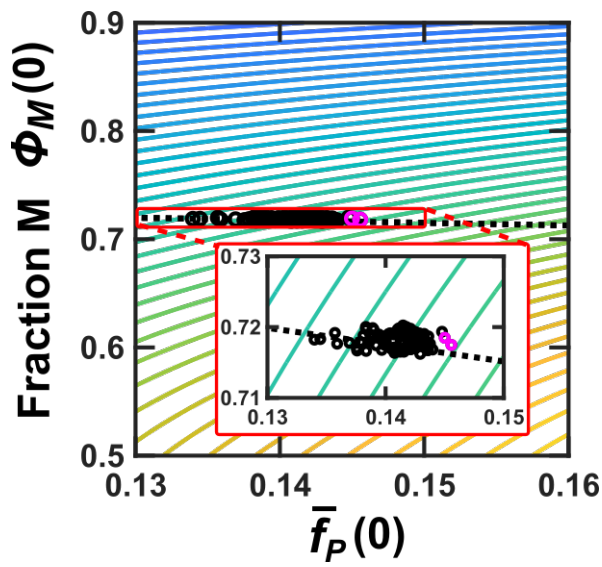

Figure 3–Figure supplement 3. Restricting fluctuations in $\phi_M(0)$ facilitates community selection. During community reproduction, we sort H and M biomass so that $\phi_M(0)$ is close to ϕ_M of the parent Adult community (similar to Figure 2). Circles mark $\overline{f}_P(0)$ and $\phi_M(0)$ of Newborn communities from a selection cycle and magenta circles mark successful Newborns. Compared to Figure 3A where circles spread over a wide interval of $\phi_M(0)$, circles here spread over $\overline{f}_P(0)$ because $\phi_M(0)$ is almost fixed. As a result, high $P(T)$ results mostly from high $\overline{f}_P(0)$, as evident by the two magenta circles having the highest $\overline{f}_P(0)$.

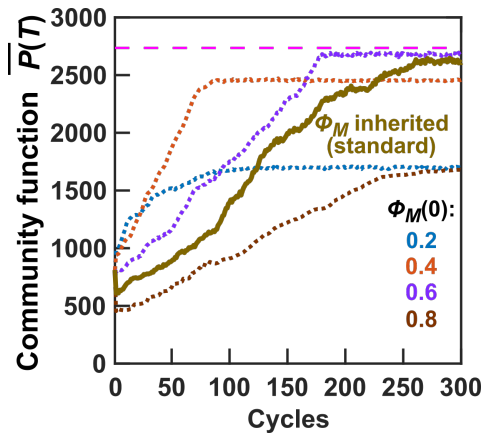

Figure 4–Figure supplement 1. Combination screening at a pre-fixed $\phi_M(0)$ can underperform or outperform standard community selection. Dynamics of standard selection (where a Newborn inherits the species composition of its parent Adult; solid) and combination screening at various fixed $\phi_M(0)$ (dotted) are plotted. As expected, when $\phi_M(0)$ is set near what is optimal for community function (0.54, Figure 1B), combination screening (purple) reaches a higher $P(T)$ than standard community selection (olive). Otherwise, the opposite is true (compare blue and brown with olive). Higher rate of community function improvement corresponds to higher density of $P(T)$ isoclines. For example, isocline density is much higher at $\phi_M(0) = 0.6$ compared to $\phi_M(0) = 0.8$ (Figure 4B). Here, Newborn total biomass $N(0)$ is fixed at 100, and each curve is the average of three independent simulations.